

Low loss silicon waveguides for the mid-infrared

Goran Z. Mashanovich,^{1,*} Milan M. Milošević,¹ Milos Nedeljkovic,¹ Nathan Owens,¹
Boqian Xiong,² Ee Jin Teo,² and Youfang Hu¹

¹Advanced Technology Institute, Faculty of Engineering and Physical Sciences, University of Surrey, Guildford, Surrey, GU2 7XH, UK

²Institute of Materials Research and Engineering, Agency for Science, Technology and Research, 3 Research Link, Singapore 117602, Singapore

*g.mashanovich@surrey.ac.uk

Abstract: Silicon-on-insulator (SOI) has been used as a platform for near-infrared photonic devices for more than twenty years. Longer wavelengths, however, may be problematic for SOI due to higher absorption loss in silicon dioxide. In this paper we report propagation loss measurements for the longest wavelength used so far on SOI platform. We show that propagation losses of 0.6-0.7 dB/cm can be achieved at a wavelength of 3.39 μm . We also report propagation loss measurements for silicon on porous silicon (SiPSi) waveguides at the same wavelength.

©2011 Optical Society of America

OCIS codes: (130.3120) Integrated optics devices; (130.3060) Infrared.

References and links

1. G. T. Reed, G. Mashanovich, F. Y. Gardes, and D. J. Thomson, "Silicon optical modulators," *Nat. Photonics* **4**(8), 518–526 (2010).
2. D.-X. Xu, M. Vachon, A. Densmore, R. Ma, S. Janz, A. Delâge, J. Lapointe, P. Cheben, J. H. Schmid, E. Post, S. Messaoudène, and J.-M. Fédéli, "Real-time cancellation of temperature induced resonance shifts in SOI wire waveguide ring resonator label-free biosensor arrays," *Opt. Express* **18**(22), 22867–22879 (2010).
3. A. L. Washburn, L. C. Gunn, and R. C. Bailey, "Label-free quantitation of a cancer biomarker in complex media using silicon photonic microring resonators," *Anal. Chem.* **81**(22), 9499–9506 (2009).
4. D. Vermeulen, T. Spuesens, P. De Heyn, P. Mechet, R. Notzel, S. Verstuyft, D. Van Thourhout, and G. Roelkens, "III-V/SOI photonic integrated circuit for FTTH central office transceivers in a PTP network configuration," in *Proceedings of 36th European Conference on Optical Communications, Vol. II* (Torino, 2010), paper Tu.5.C.2.
5. R. Soref, "Towards silicon-based longwave integrated optoelectronics (LIO)," *Proc. SPIE* **6898**, 689809, 689809-13 (2008).
6. R. Soref, "Mid-infrared photonics in silicon and germanium," *Nat. Photonics* **4**(8), 495–497 (2010).
7. R. A. Soref, S. J. Emelett, and W. R. Buchwald, "Silicon waveguided components for the long-wave infrared region," *J. Opt. A* **8**, 840–848 (2006).
8. X. Liu, J. B. Driscoll, J. I. Dadap, R. M. Osgood, Y. A. Vlasov, and M. J. Green, "Mid-infrared pulse dynamics in Si nanophotonic wires near the two-photon absorption edge," in *Conference on Lasers and Electro-Optic, Technical Digest (CD)* (Optical Society of America, 2009), paper CFR5.
<http://www.opticsinfobase.org/abstract.cfm?URI=CLEO-2009-CFR5>
9. <http://www.irphotonics.com>
10. G. T. Reed, *Silicon Photonics: The State of the Art* (Wiley, 2008).
11. V. Raghunathan, D. Borlaug, R. R. Rice, and B. Jalali, "Demonstration of a Mid-infrared silicon Raman amplifier," *Opt. Express* **15**(22), 14355–14362 (2007).
12. S. Zlatanovic, J. S. Park, S. Moro, J. M. C. Boggio, I. B. Divliansky, N. Alic, S. Mookherjee, and S. Radic, "Mid-infrared wavelength conversion in silicon waveguides using ultracompact telecom-band-derived pump source," *Nat. Photonics* **4**(8), 561–564 (2010).
13. X. Liu, R. M. Osgood, Y. A. Vlasov, and W. M. J. Green, "Mid-infrared optical parametric amplifier using silicon nanophotonic waveguides," *Nat. Photonics* **4**(8), 557–560 (2010).
14. T. Baehr-Jones, A. Spott, R. Ilic, A. Spott, B. Penkov, W. Asher, and M. Hochberg, "Silicon-on-sapphire integrated waveguides for the mid-infrared," *Opt. Express* **18**(12), 12127–12135 (2010).
15. A. Spott, Y. Liu, T. Baehr-Jones, R. Ilic, and M. Hochberg, "Silicon waveguides and ring resonators at 5.5 μm ," *Appl. Phys. Lett.* **97**(21), 213501 (2010).
16. M. M. Milošević, P. S. Matavulj, P. Y. Yang, A. Bagolini, and G. Z. Mashanovich, "Rib waveguides for mid-infrared silicon photonics," *J. Opt. Soc. Am. B* **26**(9), 1760–1766 (2009).
17. P. Y. Yang, G. Z. Mashanovich, I. Gomez-Morilla, W. R. Headley, G. T. Reed, E. J. Teo, D. J. Blackwood, M. B. H. Breese, and A. A. Bettiol, "Free standing waveguides in silicon," *Appl. Phys. Lett.* **90**(24), 241109 (2007).

18. E. J. Teo, A. A. Bettiol, M. B. H. Breese, P. Y. Yang, G. Z. Mashanovich, W. R. Headley, G. T. Reed, and D. J. Blackwood, "Three-dimensional control of optical waveguide fabrication in silicon," *Opt. Express* **16**(2), 573–578 (2008).
19. E. J. Teo, A. A. Bettiol, P. Yang, M. B. H. Breese, B. Q. Xiong, G. Z. Mashanovich, W. R. Headley, and G. T. Reed, "Fabrication of low-loss silicon-on-oxidized-porous-silicon strip waveguide using focused proton-beam irradiation," *Opt. Lett.* **34**(5), 659–661 (2009).
20. P. Y. Yang, S. Stankovic, J. Crnjanski, E. J. Teo, D. Thomson, A. A. Bettiol, M. B. H. Breese, W. Headley, C. Giusca, G. T. Reed, and G. Z. Mashanovich, "Silicon photonic waveguides for mid- and long-wave infrared regions," *J. Mater. Sci. Mater. Electron.* **20**(S1), 159–163 (2009).
21. E. D. Palik, *Handbook of Optical Constants of Solids*, Vol. 1 (Academic, 1985).
22. D. E. Aspnes, "Optical properties of thin films," *Thin Solid Films* **89**(3), 249–262 (1982).
23. G. Z. Mashanovich, W. R. Headley, M. M. Milošević, N. Owens, E. J. Teo, B. Q. Xiong, P. Y. Yang, M. Nedeljkovic, J. Anguita, I. Marko, and Y. Hu, "Waveguides for mid-infrared group IV photonics," in *Proceedings of IEEE Conference on Group IV Photonics*, (Institute of Electrical and Electronics Engineers, 2010), pp. 374–376.
24. G. T. Reed and A. P. Knights, *Silicon Photonics: An Introduction* (Wiley, 2004).
25. <http://www.photonond.com>
26. F. Y. Gardes, G. T. Reed, A. P. Knights, G. Mashanovich, P. E. Jessop, L. Rowe, S. McFaul, D. Bruce, and N. G. Tarr, "Sub-micron optical waveguides for silicon photonics formed via the local oxidation of silicon (LOCOS)," *Proc. SPIE* **6898**, 68980R, 68980R-4 (2008).
27. C. Tsay, E. Mujagić, C. K. Madsen, C. F. Gmachl, and C. B. Arnold, "Mid-infrared characterization of solution-processed As₂S₃ chalcogenide glass waveguides," *Opt. Express* **18**(15), 15523–15530 (2010).
28. C. Vigreux-Bercovici, E. Bonhomme, A. Pradel, J.-E. Broquin, L. Labadie, and P. Kern, "Transmission measurements at 10.6 μm of Te₂As₃Se₅ rib waveguides on As₂S₃ substrate," *Appl. Phys. Lett.* **90**(1), 011110 (2007).

1. Introduction

The main focus of silicon or group IV photonics research activity has been in the near-infrared (NIR) wavelength region, as a number of research groups are addressing the interconnect bottleneck [1], sensing [2,3] and fibre-to-the-home applications [4]. The mid-infrared (MIR) wavelength region has not received as much attention even though it offers a plethora of possible applications ranging from sensing, medical diagnostics, and free space communications, to thermal imaging and IR countermeasures [5].

The fact that silicon and germanium are low-loss in the MIR [6] facilitates migration of photonic circuits to this wavelength region. Furthermore, the free-carrier plasma dispersion effect should be stronger [7], two photon absorption is reduced [8], and more robust optical fibres are now available at longer wavelengths [9]. Finally, the dimensional tolerances are more relaxed for MIR devices than for those in the NIR, thus simplifying fabrication [10].

Recently, there has been an increased interest in MIR group IV photonics. Possible waveguide structures have been suggested [7], and Raman amplification in bulk silicon [11], non-linear effects in SOI around the 2 μm wavelength [12,13], and passive structures on the silicon-on-sapphire platform at 4.5 and 5.5 μm [14,15] have all been reported.

The most popular platform in the NIR, SOI, has not been considered as a candidate for wavelengths longer than 2.5 μm due to a high material loss of SiO₂. We have previously theoretically investigated MIR SOI rib waveguides [16], and in this paper we report, for the first time, experimental verification of low loss SOI waveguiding at a wavelength as long as 3.39 μm . As the 3–5 μm wavelength range is interesting due to several application areas, the results presented here could lead to the realisation of a range of MIR integrated photonic circuits on SOI platform. We also investigate another potential candidate for longer wavelengths, a silicon-on-porous silicon waveguide [17–20]. First, the design and fabrication of the two waveguide structures are described, followed by the experimental technique used in this work. Finally, the experimental results are presented.

2. Waveguide design and fabrication

It is well known from literature that silicon is relatively low loss (<2 dB/cm) for wavelengths up to 8 μm , whilst there are several multiphonon absorption peaks at longer wavelengths [21]. On the other hand, SiO₂ optical loss rapidly increases beyond 3.6 μm , and therefore SOI is not a suitable candidate for longer wavelengths. Due to this limitation, the material technology

could potentially be used for wavelengths around 3 μm , but that has never been experimentally confirmed until now.

We have designed SOI waveguides following the guidelines published in [16]. Rib waveguides with a height of 2 μm , width of 2 μm and etch depth of 1.2 μm were chosen, as their overall dimensions ensured efficient coupling from MIR optical fibres since a low power MIR laser was used in this work. In addition, nearly polarisation insensitive light propagation is achievable in these relatively large waveguides which is important as polarisation maintaining mid-infrared fibres are not yet commercially available. Standard lithography and reactive ion etching (RIE) were used in fabrication.

By replacing the oxide with a different cladding, we can potentially obtain structures that guide at longer MIR wavelengths. Such a cladding can be air or porous silicon. We have fabricated SiPSi waveguides by proton beam irradiation. We used ion irradiation with 250 keV protons and a fluence of about $1 \times 10^{14} \text{ cm}^{-2}$ [18]. After irradiation, the sample was electrochemically etched in a solution of HF:water:ethanol with a ratio of 1:1:2 and a two-step etching process was performed. The refractive index of the annealed PSi is found to be about 1.4 from fitting the reflectance spectra using the Bruggeman formula [22]. Waveguides can be fabricated by direct irradiation of Si without using a photoresist pattern, or by using a photoresist pattern with irradiation performed over a large area (Fig. 1). The latter method is preferred. Here we report on experimental results for waveguides fabricated by both methods. Relatively large dimensions of SiPSi waveguides were chosen as they allow comparison with previous measurements reported in [19]. Also, the photolithography process used in the large area irradiation of waveguides limits the resolution and size to more than 2 μm in lateral dimension. Better resolution and smaller single mode waveguides can be achieved when electron beam lithography is employed. More details concerning fabrication are given in [18,19].

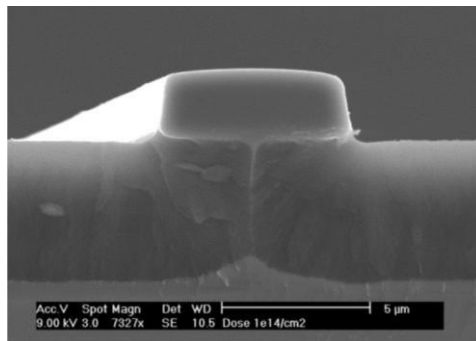


Fig. 1. Cross section of a Si on porous Si waveguide fabricated by proton beam irradiation over a large area [23].

3. Experimental setup

The measurements we undertaken by using the setup shown in Fig. 2. The source was a Thorlabs 3.39 μm , 2 mW CW linearly polarised He-Ne laser. At this wavelength Si and SiO_2 materials are low loss. Additional polarisation control was provided by two ZnSe MIR polarisers (Fig. 2). Light was coupled into a 9/125 μm single-mode MIR optical fibre [9] via a ZnSe objective lens and then it was butt coupled into the sample. Light exiting the sample was butt coupled to another single mode MIR fibre and then it was directed to a MIR detector (Infrared Associates Inc, IS-1.0). Both input and output fibres were held on 3-axis NanoMax stages from Thorlabs and adjustments could be made to their positions through piezo-controllers (MDT693A). By butt coupling the fibres to the sample, the setup was simplified. To confirm MIR light was propagating through the waveguides, a broadband NIR source (AFC Technologies Inc, BBS 15/16 D-TS) and detector (Agilent, 81264B) were introduced into the setup. A NIR camera (Hamamatsu, C2741) was used to align the sample such that

light was visible in the waveguide. After the output power was maximised on the detector, the fibre connectors were used to switch the input and output to the MIR laser and detector. Another method of confirming that MIR light was propagating thorough the waveguides, would be to implement a MIR camera [23].

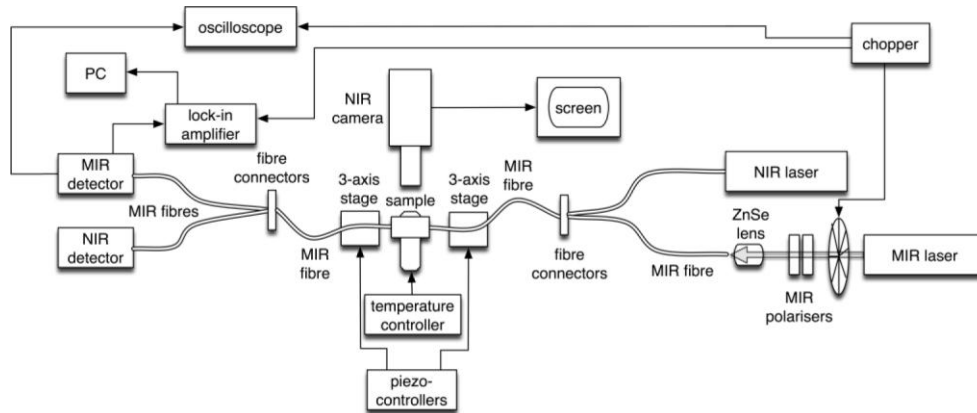


Fig. 2. Experimental setup used for measurements.

To increase the signal-to-noise ratio, a chopper and a lock-in amplifier were used. A PC was connected to the lock-in amplifier to record the data and to determine the average value and standard deviation of the signal. In order to accurately measure the output signal from the sample, we added a sample stage with a Peltier element to change the temperature of the sample and avoid a Fabry-Perot (FP) dependence of the output signal (Fig. 2).

We used the cut-back method to determine the propagation loss [24]. For the SOI waveguides, 10 μm wide tapers were positioned at the input and output to increase the coupling efficiency to the optical fibres. A bend radius of 200 μm was incorporated into the devices to minimise the bend losses. The experimentally measured bend loss was 0.006 ± 0.002 dB for a 90° bend. There were no tapers on SiPSi waveguides as they had relatively large cross section. In addition to using the Peltier element on the sample stage to control the temperature of the sample and minimise the influence of FP variations on the output signal, we tuned the temperature of the sample to estimate the propagation loss by the FP method [24] and to confirm our cut-back loss figures.

As polarisation maintaining fibres are not yet commercially available, it was not possible to determine which polarisation was coupled into the waveguides. We introduced two MIR polarisers in the setup (Fig. 2) and performed measurements for TE/TM input polarisations. It was found the waveguide propagation losses were similar. This is not surprising taking into account the design and dimensions of the waveguides tested [16,19]; therefore, it can be assumed the polarisation dependence of the propagation loss is not significant for the previously described setup and device dimensions.

4. Experimental results

Each sample was measured several times and each individual waveguide measurement was averaged over a several minute period. The averaged value and standard deviation were calculated on a PC connected to the lock-in amplifier. The error estimate is shown in the final plots presented below.

The noise floor was determined by initially maximising the detector power and then by moving the input fibre laterally out of alignment with a waveguide until the detector power had stabilized to a steady state value. The observed power was more than 20 dB lower than the typical measured peak power and the total on chip loss was around 23 dB. From modelling, coupling at each facet contributed 9 dB.

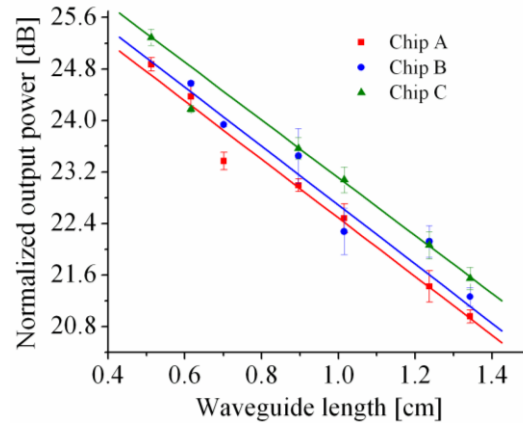


Fig. 3. Relatively high propagation losses of 4.6 ± 0.2 dB/cm (chip A), 4.5 ± 0.2 dB/cm (chip B), 4.5 ± 0.3 dB/cm (chip C) were measured for SOI samples with $1 \mu\text{m}$ BOX.

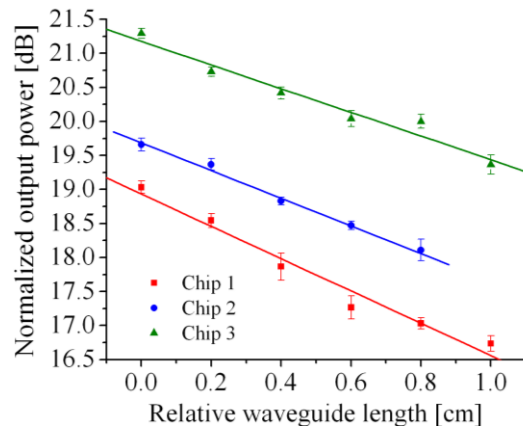


Fig. 4. Lower propagation losses of 2.4 ± 0.2 dB/cm (chip 1), 2.0 ± 0.2 dB/cm (chip 2), and 1.9 ± 0.2 dB/cm (chip 3) were measured for SOI samples with $2 \mu\text{m}$ BOX.

The first batch of devices was fabricated on SOI wafers with a $2 \mu\text{m}$ Si overlayer on $1 \mu\text{m}$ thick buried oxide (BOX). Typical measurements are shown in Fig. 3. The propagation loss of $4.5 - 4.6$ dB/cm at $3.39 \mu\text{m}$ suggested the buried oxide layer was not sufficiently thick. We simulated propagation loss dependence versus BOX thickness using FIMMWAVE [25]. The modelling confirmed a $1 \mu\text{m}$ BOX is not sufficient to suppress substrate leakage, resulting in 2 dB/cm leakage loss.

We therefore fabricated the second batch of devices on SOI wafers with a $2 \mu\text{m}$ thick BOX and we measured significantly lower losses of $1.9 - 2.4$ dB/cm (Fig. 4). As the propagation loss was still relatively high, we oxidised the waveguides with a $20\text{-}30$ nm thick thermal oxide to reduce the surface roughness. This resulted in propagation losses of $0.6 - 0.7$ dB/cm at $3.39 \mu\text{m}$ (Fig. 5).

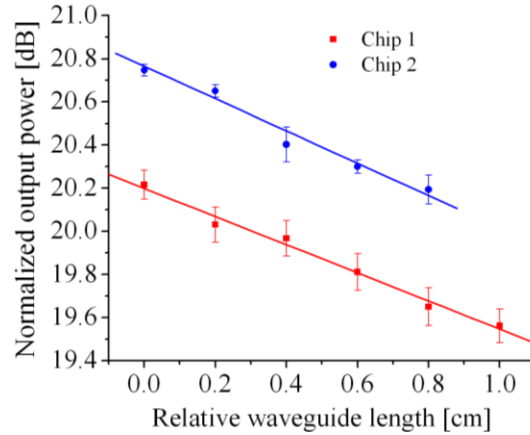


Fig. 5. SOI samples with 2 μm BOX that had around 2 dB/cm propagation loss before oxidation showed significantly lower losses after oxidation: 0.6 ± 0.2 dB/cm (chip 1), 0.7 ± 0.1 dB/cm (chip 2).

As mentioned earlier, we have performed measurements for different input polarisations and one typical example is shown in Fig. 6. It can be seen that the results for TE/TM input polarisations are very similar.

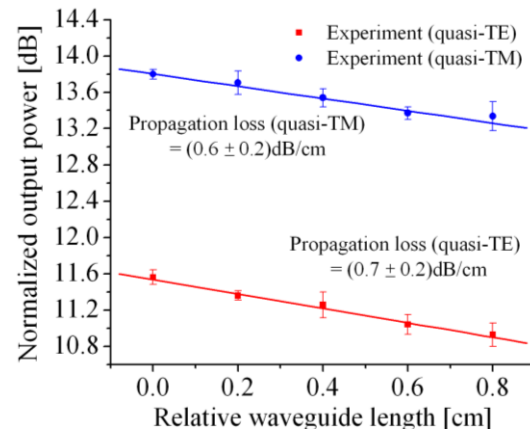


Fig. 6. Propagation loss was similar for both TE and TM input polarizations.

These results are very promising as they demonstrate, for the first time, that SOI waveguides can be low loss at this MIR wavelength. Although the SOI waveguides are relatively large we believe that sub dB/cm losses can be achieved by using even smaller structures such as for example LOCOS waveguides [26]. The propagation loss demonstrated here is also much lower than losses previously reported in the literature for other MIR waveguides [14,27,28].

Propagation losses for SiPSi waveguides fabricated by a direct write process, were around 6 dB/cm. Figure 7 shows a cut back measurement for $4 \times 2 \mu\text{m}$ SiPSi waveguide. The propagation loss for this waveguide was 5.6 ± 0.2 dB/cm. As large area irradiation is a preferred method for the fabrication of SiPSi waveguides we also performed measurements for those waveguides. These were oxidised after etching to reduce the surface roughness. Losses as low as 2.1 ± 0.2 dB/cm at $1.55 \mu\text{m}$, and 3.9 ± 0.2 dB/cm at $3.39 \mu\text{m}$ were measured for $4 \times 2 \mu\text{m}$ waveguides (Fig. 8).

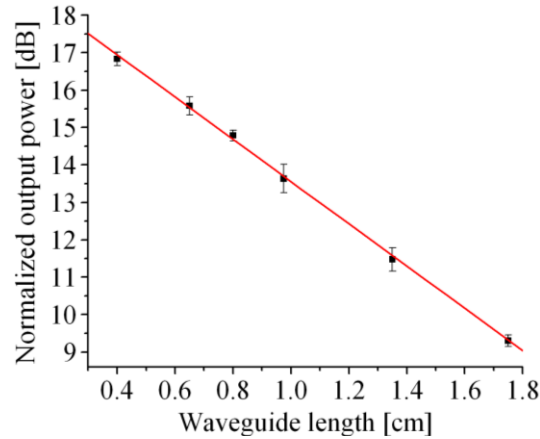


Fig. 7. Propagation loss for unoxidized $4 \times 2 \mu\text{m}$ SiPSi waveguide fabricated by the direct write method was $5.6 \pm 0.2 \text{ dB/cm}$.

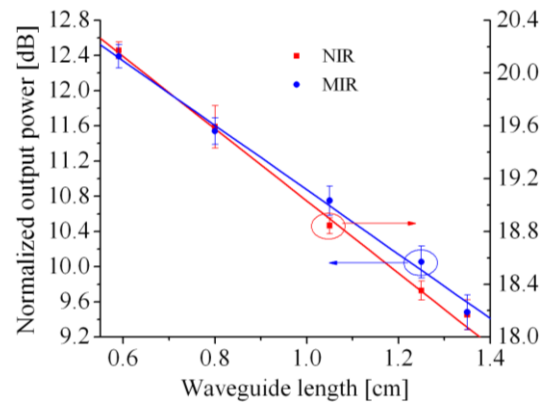


Fig. 8. Propagation loss for oxidized $4 \times 2 \mu\text{m}$ SiPSi waveguides fabricated by large area implantation: a) $2.1 \pm 0.2 \text{ dB/cm}$ at $1.55 \mu\text{m}$, and b) $3.9 \pm 0.2 \text{ dB/cm}$ at $3.39 \mu\text{m}$.

We suspect that the observed losses are mainly due to surface roughness. For longer wavelengths it can be expected that losses decrease as the ratio of the roughness amplitude to the wavelength also decreases. However, for longer wavelengths a larger proportion of the optical mode is interacting with the sidewalls thus increasing the propagation loss. For the SiPSi waveguides, the latter contribution seems to be larger than the former and hence the propagation loss at $3.39 \mu\text{m}$ is also higher. The absorption loss of porous silicon at the MIR needs also to be determined to confirm this assumption.

In addition, the SiPSi propagation loss at the wavelength of $1.55 \mu\text{m}$ is slightly larger than previously reported values of $1.4\text{--}1.6 \text{ dB/cm}$, suggesting that slight variations in the fabrication process may result in a reduction of MIR propagation loss from the current value of 3.9 dB/cm to values below 3 dB/cm . Although relatively low resistivity ($0.7 \Omega\text{cm}$) crystalline silicon is preferable for the fabrication of SiPSi waveguides, we will attempt to use silicon with higher resistivity to reduce the propagation loss without compromising the fabrication process.

5. Conclusion

In this paper, to the best of our knowledge, the first demonstration of low loss propagation of mid-infrared light at the wavelength of $3.39 \mu\text{m}$ through silicon-on-insulator waveguides has been presented. The minimum loss for $2 \mu\text{m}$ high rib SOI waveguides was $0.6\text{--}0.7 \text{ dB/cm}$.

We have also measured SiPSi structures at the same wavelength. The reason for the relatively high propagation loss (3.9 dB/cm) may be the surface roughness and the fact that low resistivity Si was used in their construction. Therefore, in the future waveguides will be fabricated on more resistive Si, and we will also optimise the oxidation process to reduce the surface roughness and further decrease the loss figures.

Results for SOI waveguides are very encouraging as they confirm that oxide is low loss for wavelengths around 3 μm . Low loss SOI waveguides can now serve as a building block for more complex passive and active MIR devices, and eventually for MIR SOI photonic circuits which will be used in a host of applications offered by this wavelength region.

Acknowledgments

Goran Mashanovich would like to acknowledge support by the Royal Society through the Royal Society Research Fellowship. Part of this work was funded by the United Kingdom Engineering and Physical Research Council (EPSRC) "UK Silicon Photonics" grant. Milan Milošević is grateful to the Higher Education Funding Council for England for the Overseas Research Studentship Award, and to the University of Surrey for the University Research Scholarship. The authors thank William Headley and Pengyuan Yang for their assistance with the measurements and sample preparation.